

A NEW ANALYSIS METHOD FOR TWO-DIMENSIONAL X-RAY DATA

Jay Hanan,^{1,2*} Ersan Üstündag,² Jonathan D. Almer³

¹*Bio-Inspired Technologies and Systems, Jet Propulsion Laboratory, Pasadena, CA 91109*

²*Department of Materials Science, California Institute of Technology, Pasadena, CA 91125*

³*Advanced Photon Source, Argonne National Laboratory, Argonne, IL 60439*

ABSTRACT

Improvements in X-ray optics and detectors have led to unprecedented challenges in interpreting diffraction information. One challenge is obtaining strain results from Debye-Scherrer rings originating from a few grains of material. In addition, results are typically desired from multiple rings over hundreds or thousands of exposures. Current two-dimensional analysis methods build on existing one-dimensional powder diffraction analysis methods. While informative, such analyses are not optimally tuned for extracting average powder-like strains from spotty or noisy rings. A two-dimensional analysis method where both 2θ and the azimuthal direction were fit simultaneously was implemented and tested on two-dimensional diffraction data taken from a synchrotron source and compared to results from more traditional one-dimensional stepwise fits to the same diffraction data. Advantages include improved fitting statistics for spotty rings, reduced susceptibility to translation error, and successful analysis in cases where the traditional methods fail.

INTRODUCTION

X-ray diffraction (XRD) has long been used in stress/strain studies. The analysis methods for determining strain with XRD have been influenced by detectors and the resulting data format [1]. In most cases, data have been collected using a point detector along a radius of a Debye-Scherrer ring providing familiar one-dimensional peak profiles. Peak shifts determined as a difference in initial and final angles, $\Delta(2\theta)$ are proportional to changes in the average distance between lattice planes, Δd [2]. It is this change in lattice spacing which provides the lattice strain from a diffraction experiment. Methods for measuring and analyzing strain using one-dimensional diffraction are well developed [3]. When area detectors became reliable, the one-dimensional analysis methods were extended to apply to the two-dimensional X-ray diffraction (XRD²) data [4, 5, 6, 7, 8, 9]. The equations for XRD² define an ellipse, which includes the distortion of the Debye-Scherrer ring caused by strain [9].

In a typical strain measurement using XRD, the sampling volume encompasses a large number of diffracting grains resulting in the so-called “powder average”. While such measurements provide useful information, many micromechanical models require spatially resolved data for comparison and validation [10, 4]. Recent advances in X-ray optics now allow spatially resolved measurements which yield data useful for such models. However, these measurements gather diffraction data from very few grains and therefore produce “spotty” Debye-Scherrer rings. The traditional one-dimensional methods are insufficient for analyzing

* Corresponding author Jay.C.Hanan@jpl.nasa.gov

This document was presented at the Denver X-ray Conference (DXC) on Applications of X-ray Analysis.

Sponsored by the International Centre for Diffraction Data (ICDD).

This document is provided by ICDD in cooperation with the authors and presenters of the DXC for the express purpose of educating the scientific community.

All copyrights for the document are retained by ICDD.

Usage is restricted for the purposes of education and scientific research.

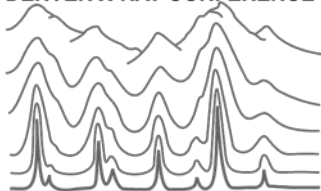
DXC Website

– www.dxcicdd.com

ICDD Website

– www.icdd.com

DENVER X-RAY CONFERENCE®



such data and yield large errors. The following describes an ellipse based two-dimensional analysis method which reduces strain error and generates useful data for micromechanical models.

EXPERIMENTAL PROCEDURE AND DATA ANALYSIS

XRD² data collected from a Ti matrix-SiC unidirectional fiber laminar composite was used to compare the two analysis methods (see Figure 3 for additional description of the sample geometry). The composite was examined using 65.3 keV X-rays (wavelength, $\lambda = 0.190 \text{ \AA}$) at the 1-ID-C beam line (SRI-CAT, Sector 1), Advanced Photon Source (APS). The diffraction data were collected with a 34.5 cm diameter digital image plate placed 1 meter downstream from the sample. A Si powder [11] was attached to the sample as an internal standard minimizing systematic errors such as the displacement error [12]. The Si powder was also used to calibrate the image plate [6]. At this energy, more than 93% of the incoming X-rays are transmitted; thus the whole thickness of the composite (200 μm) was sampled.

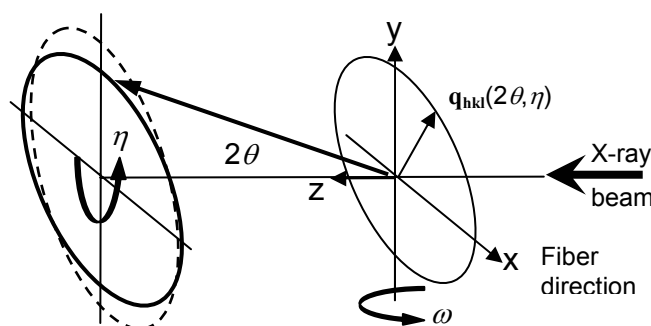


Figure 1. Scattering geometry of the experimental setup. x, y, z axes define the laboratory coordinate system. The scattering vector q and the diffracted beam for a grain are indicated. Note that all scattering vectors (coinciding on a cone) are detected simultaneously on the area detector. In this setup the SiC fibers were parallel to the x axis (for $\omega = 0^\circ$).

For a specimen perpendicular to the transmitted beam, it may be shown ([13]) that the diffraction cone will deform with strain according to:

$$(a^2 + c^2)\varepsilon_{xx} + 2ab\varepsilon_{xy} + b^2\varepsilon_{yy} = \ln \left[\frac{\sin \theta_0}{\sin \theta} \right] \quad (1)$$

Where ε denotes a component of the strain tensor in the plane perpendicular to the beam with the indices defined by the coordinate system depicted in Figure 1. Here, $a = \sin \theta$, $b = -\cos \eta \cos \theta$, $c = -\sin \eta \cos \theta$, and $\ln(\sin \theta_0 / \sin \theta)$ represents the diffraction cone distortion at a given $(2\theta, \eta)$ position with respect to a reference Bragg angle, θ_0 . Equation 1 is a simplification of the more general solution valid for any sample or detector orientation with respect to the beam [9].

An extensive model XRD² data set was collected from the Ti-SiC composite using the setup described above. The data were analyzed with two different methods. The first method converts

the polar coordinates of the diffraction pattern into Cartesian coordinates and constructs a fit to peaks along the 2θ axis. For this reason it is called the “one-dimensional” analysis. A second method leaves the data in the original coordinate system and fits the complete Debye-Scherrer ring as an ellipse. A description of each method follows.

One-Dimensional (“Traditional”) Analysis

This method is useful for determining the hkl specific two-dimensional strain tensor of multiple phases. An automated analysis, adapted from [7], was developed. It consists of three main steps:

- 1) Reduce the image plate data into a Cartesian coordinate format through a transformation based on an internal standard.
- 2) Fit the peak in 2θ at each η for all rings of interest using a least squares routine.
- 3) Solve the strain tensor using Equation 1 for each ring of interest using all peak positions from Step 2.

Typical analysis time per scan was about 5 minutes depending on the computer power and number of phases present. The analysis program was written in MatLab.[†] Initial calibration and conversion of the image plate files was performed using macros running on a software package called, Fit2D[‡] [6]. The details of each step and MatLab scripts used for this analysis are found in [4]. Strain error is based on a standard deviation of the fit assuming a Gaussian error distribution.

One drawback to this analysis is its sensitivity to outliers. Outliers are erroneous peak centers which may come from noise or neighboring rings. In one-dimensional analysis, a short range in 2θ is selected for each peak of interest. This predetermined $\Delta(2\theta) = 2\theta_{\max} - 2\theta_{\min}$ is used as a window for fitting the peak. If the peak resides outside the window, is not observed at a particular η , or a second peak enters the window, false peak positions may be recorded. This possibility limits which rings may be considered for analysis as they must be clear of neighboring rings and have sufficient intensity to provide a solution to the peak fitting routine. As the beam size is reduced, variations in intensity around the ring increase. This is due to a decrease in the number of diffracting grains in the sampling volume. In the case of highly textured minority phases, the intensity may be restricted to a small region in η . While a narrow acceptance window $\Delta(2\theta)$ may eliminate the majority of outliers, a $\Delta(2\theta)$ which is not a function of η is restricted by Poisson’s ratio to a value larger than otherwise necessary. In addition, using this “traditional” method, $\Delta(2\theta)$ must be large enough to accommodate the change in radius associated with the change in strain for the phase of interest. These restrictions result in outliers which prevent the analysis of some rings.

Resolving these restrictions requires an iterative approach to fitting the Debye-Scherrer ring as a whole. An initial guess of $2\theta_{\min}$ and $2\theta_{\max}$, cannot be based on the final solution for the fit ellipse; hence the need for an iterative approach. Determining $\Delta(2\theta)$ as a function of η and ε , allows minimization of $\Delta(2\theta)$ and the incorporation of more rings in the analysis. Including more rings is the first step to adopting a comprehensive whole pattern fitting (“Rietveld”) approach to analyzing XRD² data.

[†]MatLab© is commercially available from The MathWorks, Inc., 3 Apple Hill Drive, Natick, MA 01760-2098.

[‡]Fit2D is freely distributed software available from: <http://www.esrf.fr/computing/scientific/FIT2D/index.html>.

Ellipse Based Two-Dimensional Analysis

The following ellipse fitting method resolves some of the limitations of the above one-dimensional analysis. One area of improvement for this new method is its ability to work directly from the raw data. Since no conversion to Cartesian coordinates is required, errors associated with this step are eliminated [6]. As discussed above, reducing the active window (mask) around a ring, allows analysis of rings that may possess close neighboring rings from other phases. The ellipse method naturally provides for a mask about an envelope described by the following ellipse equation:

$$Ax^2 + Bxy + Cy^2 + Dx + Ey + F = 0 \quad (2)$$

Where previously, particularly under high anisotropic strain, the mask would have to remain large; the elliptical mask is iteratively matched to the best solution for the strain given by the ring, minimizing the effects of neighboring phases. For example, a mask may be applied to a given ring in exposure no. 2 (R_2) based on a solution to the same ring in exposure no. 1 (R_1). If the solution to R_1 is different than that to R_2 , then R_1 's mask will be slightly off center for R_2 . Therefore, the procedure is to first solve R_2 based on R_1 , and then recreate the mask based on the new fit to R_2 . A second iteration of the fit to R_2 using the updated mask removes potential influences from the specifics of R_1 's mask. This may be repeated until no changes in the mask are observed.

Since "peak centers" from a profile peak shape fit to the intensity across the ring are not used in this analysis, the pixel intensity directly restricts the parameters of the fitted ellipse. Since the pixel intensity (I) for the ring is observed across $\Delta(2\theta)$, the ellipse must be fit across three dimensions (θ , η , and I). To produce a three-dimensional solution from a two-dimensional fit, the pixels in each Debye-Scherrer ring are divided into weighted layers of intensity. As with the previous method, a Matlab program is used to solve a least squares best fit of Equation 2 to each intensity layer according to its weight [14]. The weighted average solution is reported as the best fit ellipse for that ring. Iterative solutions for the same ring may be performed since the mask is directly dependent on the best guess for the fit to the ring. For situations where changes in strain are expected, the solutions are performed in order where the difference between solutions for neighboring exposures is small. A standard deviation for the weighted data layers is also calculated for each ellipse providing an estimate for the error in strain. If the loading axis is known, longitudinal and transverse strain may be taken from the change in the intercept of the best fit ellipse along the loading axis and the axis perpendicular to it. Intrinsic to the analysis is a recalculation of beam center with each fit which minimizes error from potential movement of the area detector. Ellipse fits to the internal standard (Si) may be used to observe and correct potential errors. Strain observed from the internal standard is assumed false and subtracted from the strain observed in the stressed phases.

RESULTS AND DISCUSSION

As hypothesized, the ellipse based method shows an improvement over the traditional method. This is best observed through a strain error dependence on the beam size to grain size ratio (average beam width / average grain diameter). This dependence is clearly apparent using the traditional linear methods and is not as significant when using the ellipse fitting method (**Figure 2**). The fitting error for the two methods converge as the beam size to grain size ratio

exceeds 100. Below 100 the fitting error may be cut by more than half when using the ellipse method.

A comparison of the results from a $500 \times 500 \mu\text{m}^2$ beam experiment by the two methods shows that within the error of the analysis, the same value for the “effective” Young’s modulus is obtained from each: 236 GPa and 226 GPa for SiC (220) via method 1 and 2, respectively, and 184 GPa and 191 GPa for Ti (10.2) from method 1 and 2, respectively. This is only a 4% difference between the results from each method. Notice, however, the error observed from the larger grained phases is reduced by 75% when the elliptical analysis is performed (Figure 2). Since the rings produced by the fine grained SiC are smooth, both analyses should give similar results.

When a small ($90 \times 90 \mu\text{m}^2$) beam size was used to study spatially resolved damage evolution in Ti-SiC composites a significant improvement in the strain error was observed: from $200 \mu\epsilon$ to $50 \mu\epsilon$ error in the Ti strain data. In addition, diffraction data previously inaccessible using the traditional method could be analyzed successfully with the ellipse method (Figure 3). The new method’s tolerance to overexposure allowed the analysis of these data. These strains compare favorably to strains measured on a later unstressed configuration of this sample using the linear analysis method published earlier [4, 5, 13].

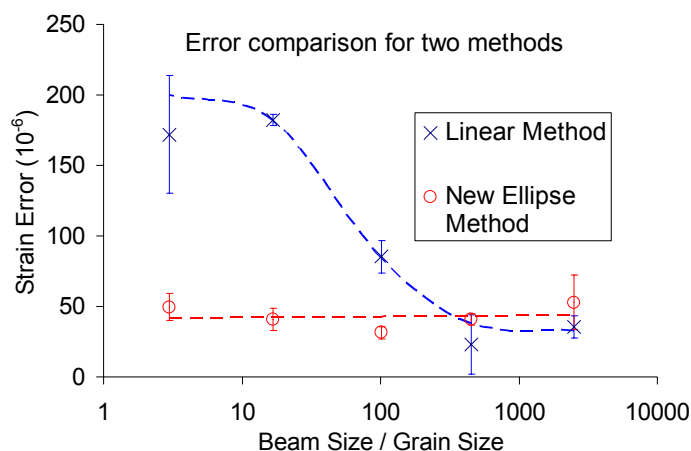


Figure 2. Error given by each analysis method as a function of beam size to grain size ratio, a measure of the number of grains contributing to the diffraction pattern. Fitting the entire ellipse at once shows significantly less increase in error as the number of contributing grains decreases. As many as 500 measurements contribute to each point in the graph. The distribution of strain values is given by the error bars depicting the standard deviation of the available data. The beam size used ranged from $500 \times 500 \mu\text{m}^2$ (*macrobeam*) to $90 \times 90 \mu\text{m}^2$ (*microbeam*) while the phases analyzed included the following (numbers in parentheses indicate average grain size): Ti (30 μm), Si (5 μm) and SiC (0.2 μm).

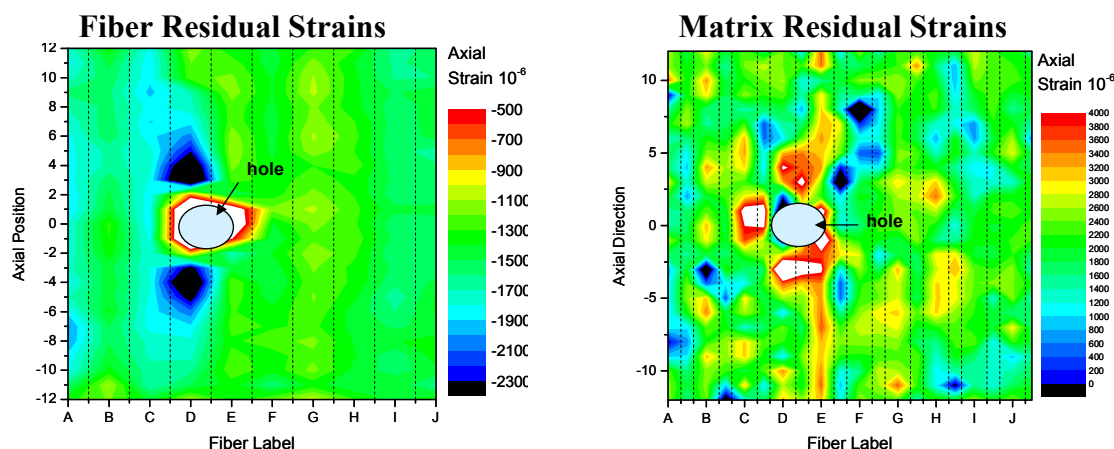


Figure 3. Contours of *residual strain* from the ellipse analysis method of microbeam measurements on the Ti-SiC composite. Due to streaks in the image plate from overexposure, the raw data could only be analyzed with the new ellipse analysis. The fibers (diam.=140 μm) are spaced 100 μm apart parallel to the grid lines in the axial direction. Fiber centers are labeled with letters A-J. A hole was introduced in the middle to initiate damage so that its evolution under applied tensile stress (along fiber axes) could be studied.

One difference between the two methods is the number of fitting parameters required. The linear method employs more parameters since each η slice is fitted separately. In our case, there are 120 individual peak profile fits per ring before fitting the peak centers to Equation 1. The advantage in the ellipse method is that the fit is directly for an ellipse—a function of η and θ , rather than a function of η , which is a function of θ , or simply $f(\eta, \theta)$ vs. $f(\theta(\eta))$.

A disadvantage of the ellipse fitting method includes the slower rate of processing. Since the entire image plate serves as raw data to the analysis, a large matrix must be kept in memory for analysis. In our case, the ellipse method used 250,000 pixels per ring where the linear method used only 7200. To compensate for the computational demand, the 17 bit dynamic intensity range was binned at a scale equivalent to the background intensity (on the order of 1000 intensity bins showed satisfactory performance). In addition, with automation, the ellipse analysis can be left to calculate over day, night, and weekends, freeing the researcher to other tasks. Some automation was available to the linear method, but in practice, since it is performed in multiple steps, it demands close attention. Furthermore, the existence of multiple steps in an analysis provides an additional source for error.

SUMMARY

A new analysis method was developed that fits entire Debye-Scherrer rings. This method is noise tolerant and enables two-dimensional strain analysis with smaller sampling volumes achieved with X-ray microdiffraction. However, the new analysis is numerically more demanding than other methods. On the other hand, it can easily be automated. Both the traditional linear and new ellipse methods have value and should be applied depending on the experimental conditions.

ACKNOWLEDGEMENTS

This study was supported by the National Science Foundation (CAREER grant no. DMR-9985264) at Caltech. The work at the Advanced Photon Source was supported by the US Department of Energy, Office of Basic Energy Sciences (contract no. W-31-109-ENG-38). The authors are grateful to Benjie Limketkai for assistance in the MatLab analyses.

REFERENCES

- [1] He, B. B., *Powder Diffraction*, **2003**, 18(2), 71-85.
- [2] Cullity, B. D., *Elements of X-Ray Diffraction*. 2nd ed. Addison Wesley, Massachusetts, PA, 1978, 130, 464-475.
- [3] Noyan, I. C., Cohen, J. B., *Residual Stress*. Springer-Verlag, New York, 1987.
- [4] Korsunsky, A. M., Wells, K. E., Withers, P. J., *Scripta Materialia*, **1998**, 39 (12), 1705–1712.
- [5] Hanan, J. C., *Thesis*, Caltech **2002**.
- [6] Hammersley, A. P. *ESRF Internal Report*, **EXP/AH/95-01**, FIT2D V5.18 Reference Manual V1.6, **1995**.
- [7] Almer, J., Lienert, U., *Unpublisted document* for the Neutron / Synchrotron Summer School, Argonne National Laboratory, **2001**.
- [8] Vogel, S., *Diplomarbeit*, Christian-Albrechts-Universität zu Kiel, **2001**.
- [9] He, B. B., Smith, K. L., *Proceedings of the SEM Spring Conference on Experimental and Applied Mechanics*, Houston, TX, **1998**, 217.
- [10] Beyerlein, I. J., Landis, C. M., *Mechanics of Materials*, **1999**, 31 (5), 331-350.
- [11] NIST Spec Sheet http://patapsco.nist.gov/srmcatalog/common/view_cert.cfm?srm=640c
- [12] Wanner, A. and Dunand, D., *Metall. Mater. Trans. A*, **2000**, 31A, 2949.
- [13] Hanan, J. C., Üstündag, E., Beyerlein, I. J., Swift, G. A., Almer, J. D., Lienert U., Haefner, D. R., *Acta Mater.*, **2003**, 51, 4239-4250.
- [14] Pilu, M., Fitzgibbon, A., Fisher, R., *IEEE International Conference on Image Processing*, Lausanne, **1996**.